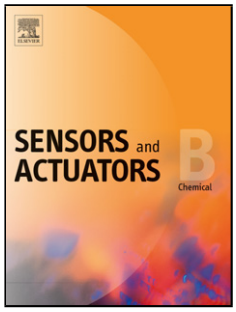


Title: Label-Free Optical Monitoring of Proteolytic Reaction Products Using Nanoporous Silica Colloidal Assembly

Authors: Giorgi Shtenberg, Naama Massad-Ivanir, Amir Khabibullin, Ilya Zharov, Ester Segal

PII: S0925-4005(18)30333-2
DOI: https://doi.org/10.1016/j.snb.2018.02.057
Reference: SNB 24152

To appear in: *Sensors and Actuators B*

Received date: 2-10-2017
Revised date: 4-2-2018
Accepted date: 6-2-2018

Please cite this article as: Giorgi Shtenberg, Naama Massad-Ivanir, Amir Khabibullin, Ilya Zharov, Ester Segal, Label-Free Optical Monitoring of Proteolytic Reaction Products Using Nanoporous Silica Colloidal Assembly, Sensors and Actuators B: Chemical https://doi.org/10.1016/j.snb.2018.02.057

# Label-Free Optical Monitoring of Proteolytic Reaction Products Using Nanoporous Silica Colloidal Assembly

Giorgi Shtenberg,[1] Naama Massad-Ivanir,[2] Amir Khabibullin,[3] Ilya Zharov,*[,3] and Ester Segal*[,2,4]

[1]Institute of Agricultural Engineering, ARO, The Volcani Center, Bet Dagan 50250, Israel
[2]Department of Biotechnology and Food Engineering, Technion – Israel Institute of Technology, Haifa 32000, Israel.
[3]Department of Chemistry, University of Utah, Salt Lake City, UT 84112, USA
[4]The Russell Berrie Nanotechnology Institute, Technion – Israel Institute of Technology, Haifa 32000, Israel

**Corresponding Authors**

*E-mail: esegal@tx.technion.ac.il
*E-mail: i.zharov@utah.edu

## Table of Contents/Abstract Graphic

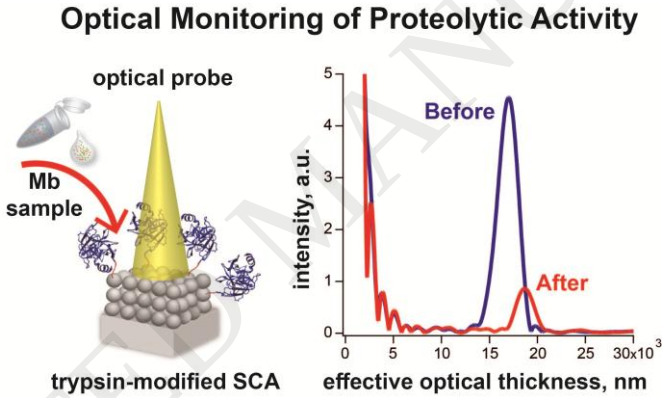


## Highlights

- Label-free optical biosensor based on multifunctional silica colloidal assembly (SCA)
- Effective optical thickness is highly sensitive to biomolecules within the nanostructure
- SCA acts as a size-exclusion element to entrap and to concentrate enzymatic degradation products
- Biosensor can be coupled to downstream mass spectrometry analysis

**ABSTRACT:** An optical biosensor for rapid monitoring of proteolytic activity is constructed by immobilization of proteases onto multifunctional silica colloidal assembly (SCA). The SCA serves as Fabry-Pérot thin film, which is highly sensitive to the presence of biomolecules (e.g., enzymes, proteins and short peptides) within the nanostructure. Moreover, the SCA acts as a size-exclusion element, allowing to entrap and to concentrate the enzymatic degradation products for downstream mass spectrometry analysis for substrate profiling and cleavage sites identification.

**KEYWORDS:** *Biosensors, Colloidal Assembly, Enzyme, Protease, Mass Spectrometry, Silica,*

### 1. Introduction

Silica colloidal crystals have been recently used in a variety of applications including drug delivery systems, chemical sensors, biological nanoreactors and bioseparations [1-6]. These emerging applications are facilitated by the ability to selectively control the molecular transport within the highly porous nanostructure of silica colloidal crystals by modifying their surface and by varying the pore size, which can be achieved by changing the nanosphere diameter [7]. Colloidal crystals are produced by self-assembly of silica nanospheres into a close-packed face-centered cubic (*fcc*) lattice, presenting a highly ordered three-dimensional (3D) array with interconnected nano-scale pores [8-10]. These tunable architectures are attractive for the construction of versatile platforms for optical biosensing applications [1, 2, 11, 12].

In the present work, we describe the design and fabrication of a simple optical biosensing platform based on silica colloidal assembly (SCA) that offers rapid monitoring of proteolytic activity. Identifying protease substrate repertoire is important for understanding the functions of protease enzymes, revealing their biological roles, and generating lead compounds for new therapies [13-16]. As a proof of concept, trypsin, one of the most widely used enzymes for peptide mapping [17], was immobilized onto the suryface of the SCA using standard silane chemistry. Specific interaction of protein substrates with trypsin molecules produced short peptides that infiltrated into the SCA nanostructure, which acted as Fabry-Pérot thin film [18]. This immediately translated into a shift in the reflectivity spectrum of the SCA, owing to the change in their effective optical thickness (EOT) [19]. The latter equals $2nL$, where $n$ is the effective refractive index of the porous film and $L$ is its physical thickness [20, 21]. Subsequently, the retrieved proteolytic reaction products were analyzed by common proteomic methods for substrate profiling and cleavage site identification.

## 2. Fabrication

In order to prepare the nanoporous SCA films, 230±20 nm silica spheres, synthesized using the Stöber method [22], were assembled into ordered colloidal films by vertical deposition onto a silicon wafer substrate. Figure 1 presents high-resolution scanning electron microscopy (HRSEM) images of a typical SCA and Figure S1 (Supplementary Material) depicts the corresponding image of the film. The cross-sectional micrograph of the SCA shows ~ 5 μm thick film, comprising of close-packed silica spheres. The film is characterized by a nanoporous structure with interconnecting interstitial spaces. The top-view micrograph (inset Figure 1) reveals the void space between the hexagonal closely packed silica spheres, which may allow infiltration of molecules/biomolecules into the SCA porous structure. It should be noted that occasional point defects within the *fcc* nanostructure were present, but did not persisted beyond one or two layers of the SCA [23]. Additional information as noted in the text is in the Supplementary material section.

## 3. Results and discussion

The optical properties of the resulting SCA were investigated using reflective interferometric Fourier transform spectroscopy (RIFTS) [24]. The film was fixed in a custom-designed cell to assure that the reflectivity was collected at the same spot during all the measurements. RIFTS is highly sensitive to small changes in the average refractive index of the thin-film, allowing for direct and real-time monitoring the binding/infiltration of different species to the pore walls/voids [20, 25-28]. A change in the average refractive index, e.g., infiltration of enzymatic reaction products or/and binding of target analyte onto the porous scaffold, leads to a red shift in the observed reflectivity spectrum that correlates with EOT changes [21, 29].

To demonstrate the applicability of the SCA as an optical sensor platform it was exposed to a model analyte solution (5 μL ethanol), which immediately resulted in a significant reflectivity spectra change (Figure 2a), that correlates to an EOT increase from $EOT_{air}$ 16,990 nm to $EOT_{EtOH}$ 18,690 nm (Figure 2b). The resulting EOT increase provided a direct measurement of the pore filling, which confirmed the SCA's potential as an optical platform for biosensing applications [1, 2].

Once the optical properties of the SCA thin-film were validated, we anchored enzymes onto the surface of SCA using a well-established methodology.[30] Briefly, SCA was first aminated by 3-aminopropyl-(triethoxyl)silane (APTES), see Figure 3b, with the aid of an organic base, diisopropylethylamine, followed by treatment with glutaric di-aldehyde (GluAld) to obtain an activated surface (Figure 3c). In the final step, primary amines on the exterior of trypsin or horseradish peroxidase were used for the immobilization onto the surface via the second reactive group of the GluAld (Figure 3d). Trypsin, one of the biologically relevant proteases for peptide mapping [17, 18], was selected as a model protease enzyme.

It should be noted that the SCA film allows proper infiltration of the biomolecules into the colloidal nano-scale pores (Figure 1, inset) [4]. Thus, it is expected that the chemical modification of the SCA surface will induce a red shift in the EOT, upon introducing different species onto the nanostructure [19]. Indeed, Figure 3e shows significant relative EOT changes after each of the described immobilization steps (APTES, GluAld and trypsin that are

normalized with respect to the EOT value of the unmodified SCA,) revealing the sensitivity of RIFTS technique as a rapid, simple and label-free detection method for small molecules as well as biomacromolecules [21]. The immobilization of the enzyme molecules onto the SCA was also confirmed by the fluorescence labeling followed by observation of the surfaces under a fluorescence microscope (see Figure S2 in the Supporting Information for details).

Once we showed that a successful biofunctionalization was achieved, we investigated the catalytic activity of trypsin by introduction of a fluorescently-labeled substrate and subsequent confocal laser scanning microscopy (CLSM) imaging. Trypsin-modified SCA was exposed to fluorescein thiocarbamoyl-labeled casein (FTC-casein) solution, allowed to react for 30 min, thoroughly washed and monitored under the microscope. As a control, horseradish peroxidase (HRP), a non-protease enzyme, was immobilized onto the SCA and the resulting film was subjected to a similar FTC-casein treatment. Figure 4 shows CLSM 3D projection images of both enzyme-modified SCA following their exposure to fluorescein-tagged substrate and the fluorescence intensity values calculated by image analysis of the CLSM data. The CLSM projection was conducted in the *z* direction from the upper surface into the pores over the depth of ~ 5 µm with a scanning step of 0.35 µm. Figure 4a shows significant fluorescence intensity throughout the entire volume of the porous scaffold, revealing that the proteolytic enzymes remain catalytically active by producing digestion products (FTC-casein peptides), and releasing fluorescence quenching on the substrate initial state [31]. The CLSM image of the HRP-modified SCA (Figure 4b) depicts insignificant fluorescence of the substrate. The calculated fluorescence intensity values for trypsin-modified SCA is 5-fold higher than that for the control, HRP-modified SCA (Figure 4c), confirming that the selectivity and the sensitivity of the conjugated proteases are preserved following surface immobilization.

Next, we demonstrate the application of our label-free RIFTS technique for monitoring the catalytic activity of trypsin. Trypsin-modified SCA was incubated with a substrate solution (i.e., myoglobin) while reflectivity spectra were collected at different time points and the corresponding EOT values were calculated. Figure 5a shows the relative EOT changes upon myoglobin introduction onto trypsin-modified SCA at two-time periods (following 1 and 2 h of incubation in room temperature). A red shift in the relative EOT is observed (Figure 5a) and a significant increase in the EOT with time, providing a direct measure of the digestion products and the myoglobin concentration inside the porous scaffold. For the control HRP-modified SCA (non-protease enzyme), exposed to a similar myoglobin solution, a small increase in the EOT values after 1 h of incubation (Figure 5a), resulting from myoglobin infiltration and adsorption unto the SCA nanostructures [18], while further incubation induced no significant EOT changes with respect to the previous step (t-test, $p>0.05$), as opposed to the trypsin reaction with the substrate (t-test, $p<0.05$). These results show that that the second increase in the EOT for trypsin-modified SCA can be attributed to the accumulation of the digestion products within the nanostructure, a result absent for the control HRP-modified SCA, as no fragments were obtained, demonstrating the specificity of our biosensor for monitoring proteolytic activity by RIFTS technique. Next, both of the enzyme-modified SCA were thoroughly washed HEPES (4-(2-hydroxyethyl)-piperazine-1-ethanesulfonic acid) buffer to retrieve myoglobin residuals, which resulted in a blue shift in the relative EOT. HRP-modified SCA showed a complete removal of myoglobin and its fragments from the nanostructure, as the corresponding EOT returned to its initial values (after enzyme immobilization, t-test, $p>0.05$). On the other hand, the EOT value for trypsin-modified SCA following buffer did not return to its initial value (t-test, $p<0.05$), which we attribute to the presence and entrapment of residual digestion products within the porous scaffold [18, 24]. These results clearly demonstrate the simplicity of our biosensing platform to monitor the retrieval of the generated peptides form the SCA for downstream/consecutive analysis.

Finally, the myoglobin peptide fragments generated in the previous experiment (trypsin-modified SCA reaction followed by buffer wash) were sequence identified by proteomic analysis by liquid chromatography-tandem mass spectrometry (LC-MS/MS) to determine substrate specificity and identify the protease's cleavage sites. Figure 5b shows distinctive sequence results of myoglobin peptide fragments after trypsin digestion under native conditions. As expected, all identified peptides contain lysines and arginines in their *N*-terminal according to the trypsin cleavage profile. While for the samples collected from the washing step of HRP-modified SCA, no peptides were detected. These results are in agreement with the RIFTS experiments, highlighting our protease-immobilized biosensing platform as a general experimental methodology that can be coupled prior to downstream MS proteomic analysis [18, 32].

## 4. Conclusion

An optical biosensing platform was designed for label-free detection of enzymatic activity of proteases, using a simple and portable experimental setup. We used a silica colloidal assembly as Fabry-Pérot thin film, which is highly sensitive to the presence of small and/or biomacromolecules within the highly porous nanostructure. For biosensor design, the SCA may present a major advantage over conventional techniques by selectively controlling the molecular

transport within the nanostructure (i.e., by acting as a size-exclusion element), which may allow entrapping and collecting the proteolytic reaction products prior to downstream proteomic analysis. The "proof-of-concept" biosensing scheme presented in this work can be further extended as a generic screening methodology of diverse enzymes, for example to analyze various proteases of interest.

**Acknowledgments**

This work was supported in part by the Lorry I. Lokey Interdisciplinary Center for Life Sciences and Engineering and with additional funding from RBNI. G.S. acknowledges the RBNI Excellence Scholarship Award. A.K. and I.Z. are grateful for support by the National Science Foundation (CHE-1710052) and by the NSF MRSEC (DMR-1121252) Seed Grant.

**References**

[1] S.-H. Kim, G.-R. Yi, Colloidal Photonic Crystals for Sensor Applications, in: M.J. Serpe, Y. Kang, Q.M. Zhang (Eds.), Photonic Materials for Sensing, Biosensing and Display Devices, Springer International Publishing, Cham, 2016, pp. 51-78.
[2] W. Chen, Z. Meng, M. Xue, K.J. Shea, Molecular imprinted photonic crystal for sensing of biomolecules, Mol Imprinting, 4 (2016) 1-12.
[3] H.R. Culver, J.R. Clegg, N.A. Peppas, Analyte-Responsive Hydrogels: Intelligent Materials for Biosensing and Drug Delivery, Acc Chem Res, 50 (2017) 170-8.
[4] I. Zharov, A. Khabibullin, Surface-Modified Silica Colloidal Crystals: Nanoporous Films and Membranes with Controlled Ionic and Molecular Transport, Acc Chem Res, 47 (2014) 440-9.
[5] J. Ding, J. Yao, J. Xue, R. Li, B. Bao, L. Jiang, et al., Tumor-homing cell-penetrating peptide linked to colloidal mesoporous silica encapsulated (-)-epigallocatechin-3-gallate as drug delivery system for breast cancer therapy in vivo, ACS Appl Mater Interfaces, 7 (2015) 18145-55.
[6] K. Watanabe, H. Ishii, M. Konno, A. Imhof, A. van Blaaderen, D. Nagao, Yolk/shell colloidal crystals incorporating movable cores with their motion controlled by an external electric field, Langmuir, 33 (2017) 296–302.
[7] A. Stein, F. Li, N.R. Denny, Morphological Control in Colloidal Crystal Templating of Inverse Opals, Hierarchical Structures, and Shaped Particles†, Chem Mater, 20 (2007) 649-66.
[8] A. Khabibullin, I. Zharov, Responsive Nanoporous Silica Colloidal Films and Membranes, Intelligent Stimuli-Responsive Materials, John Wiley & Sons, Inc.2013, pp. 265-91.
[9] É. Duguet, C. Hubert, C. Chomette, A. Perro, S. Ravaine, Patchy colloidal particles for programmed self-assembly, C R Chim, 19 (2016) 173-82.
[10] Z. Cai, N.L. Smith, J.-T. Zhang, S.A. Asher, Two-dimensional photonic crystal chemical and biomolecular sensors, Anal Chem, 87 (2015) 5013-25.
[11] A. Mocanu, E. Rusen, A. Diacon, Optical Properties of the Self-Assembling Polymeric Colloidal Systems, Int J Polym Sci, 2013 (2013) 1-11.
[12] Y.-L. Ko, H.-P. Tsai, K.-Y. Lin, Y.-C. Chen, H. Yang, Reusable macroporous photonic crystal-based ethanol vapor detectors by doctor blade coating, J Colloid Interface Sci, 487 (2017) 360-9.
[13] P. Kasperkiewicz, M. Poreba, K. Groborz, M. Drag, Emerging challenges in the design of selective protease substrates, inhibitors and activity-based probes for indistinguishable proteases, FEBS J, (2017).
[14] M.A. Pethe, A.B. Rubenstein, S.D. Khare, Large-scale Structure-based Prediction and Identification of Novel Protease Substrates using Computational Protein Design, J Mol Biol, 429 (2017) 220-36.
[15] N.J. Agard, J.A. Wells, Methods for the proteomic identification of protease substrates, Curr Opin Chem Biol, 13 (2009) 503-9.
[16] B. Turk, Targeting proteases: successes, failures and future prospects, Nat Rev Drug Discovery, 5 (2006) 785-99.
[17] T. Šlechtová, M. Gilar, K. Kalíková, S.M. Moore, J.W. Jorgenson, E. Tesařová, Performance comparison of three trypsin columns used in liquid chromatography, J Chromatogr A, 1490 (2017) 126-32.
[18] G. Shtenberg, N. Massad-Ivanir, O. Moscovitz, S. Engin, M. Sharon, L. Fruk, et al., Picking up the Pieces: A Generic Porous Si Biosensor for Probing the Proteolytic Products of Enzymes, Anal Chem, 85 (2013) 1951-6.
[19] G. Shtenberg, N. Massad-Ivanir, L. Fruk, E. Segal, Nanostructured Porous Si Optical Biosensors: Effect of Thermal Oxidation on Their Performance and Properties, ACS Appl Mater Interfaces, 6 (2014) 16049-55.
[20] C.K. Tsang, T.L. Kelly, M.J. Sailor, Y.Y. Li, Highly Stable Porous Silicon–Carbon Composites as Label-Free Optical Biosensors, ACS Nano, 6 (2012) 10546-54.
[21] M.M. Orosco, C. Pacholski, M.J. Sailor, Real-time monitoring of enzyme activity in a mesoporous silicon double layer, Nat Nanotechnol, 4 (2009) 255-8.
[22] W. Stöber, A. Fink, E. Bohn, Controlled Growth of Monodispersed Spheres in the Micron Size Range, J Colloid Interface Sci 26 (1968) 62-9.
[23] P.A.A. Ignacio-de Leon, I. Zharov, Size-selective molecular transport through silica colloidal nanopores, Chem Commun, 47 (2011) 553-5.
[24] C. Pacholski, M. Sartor, M.J. Sailor, F. Cunin, G.M. Miskelly, Biosensing using porous silicon double-layer interferometers: reflective interferometric Fourier transform spectroscopy, J Am Chem Soc, 127 (2005) 11636-45.

[25] M. Nemati, A. Santos, T. Kumeria, D. Losic, Label-Free Real-Time Quantification of Enzyme Levels by Interferometric Spectroscopy Combined with Gelatin-Modified Nanoporous Anodic Alumina Photonic Films, Anal Chem, 87 (2015) 9016-24.
[26] R. Vilensky, M. Bercovici, E. Segal, Oxidized porous silicon nanostructures enabling electrokinetic transport for enhanced dna detection, Adv Funct Mater, 25 (2015) 6725-32.
[27] A. Andres-Arroyo, B. Gupta, F. Wang, J.J. Gooding, P.J. Reece, Optical manipulation and spectroscopy of silicon nanoparticles exhibiting dielectric resonances, Nano lett, 16 (2016) 1903-10.
[28] F.S.H. Krismastuti, A. Cavallaro, B. Prieto-Simon, N.H. Voelcker, Toward Multiplexing Detection of Wound Healing Biomarkers on Porous Silicon Resonant Microcavities, Adv Sci, (2016).
[29] Y. Zhao, G. Gaur, S.T. Retterer, P.E. Laibinis, S.M. Weiss, Flow-through porous silicon membranes for real-time label-free biosensing, Anal Chem, 88 (2016) 10940-8.
[30] B. Xia, S.J. Xiao, D.J. Guo, J. Wang, M. Chao, H.B. Liu, et al., Biofunctionalisation of porous silicon (PS) surfaces by using homobifunctional cross-linkers, J Mater Chem, 16 (2006) 570-8.
[31] J.-P. Goddard, J.-L. Reymond, Enzyme assays for high-throughput screening, Curr Opin Biotechnol, 15 (2004) 314-22.
[32] S. Slamnoiu, C. Vlad, M. Stumbaum, A. Moise, K. Lindner, N. Engel, et al., Identification and Affinity-Quantification of ß-Amyloid and α-Synuclein Polypeptides Using On-Line SAW-Biosensor-Mass Spectrometry, J Am Soc Mass Spectrom, 25 (2014) 1472-81.

**Biographies**

**Giorgi Shtenberg** completed his PhD in 2014 in Biotechnology and Food Engineering at Technion–Israel Institute of Technology. He is currently a Scientist and Head of Bio-Nano-Laboratory at Institute of Agriculture Engineering, ARO-The Volcani Center. He is focusing on the development of novel biosensors/bioassays that will transform from a laboratory-based research into real on-site "lab-on-chip" platforms for addressing problems in fields of agriculture, animal diagnostics, food safety and environmental monitoring and detection.

**Naama Massad-Ivanir** received her B.Sc.degree in Biotechnology and Food Engineering from the Technion in 2006. She joined the Segal Lab on October 2007 and received her PhD in 2013. She is currently the manager of Prof. Ester Segal's lab.

**Amir Khabibullin** received his MS from Kazan Federal University in Russia and his PhD from the Chemistry Department, University of Utah, in 2014. He currently works as a scientist at Exova in Canada.

**Ilya Zharov** is an Associate Professor at the Chemistry Department, University of Utah, which he joined in 2003. He obtained his BS in 1990 from Chelyabinsk State University, his MS in 1994 from the Technion, and his PhD in 2000 from the University of Colorado, Boulder. In 2000-2003 he was a Beckman Postdoctoral Fellow at the Beckman Institute for Advanced Science and Technology, University of Illinois at Urbana-Champaign. His research focuses on novel nanoporous materials, ion conductive membranes, and on theranostic agents.

**Ester Segal** earned her BSc (cum laude) in chemical engineering in 1997 from the Technion – Israel Institute of Technology. Her PhD in polymer science was completed in 2004 at the Technion and she was awarded with the Rothschild Postdoctoral Fellowship to work at the Department of Chemistry and Biochemistry at the University of California, San Diego. In 2007 she returned to Israel and joined the Department of Biotechnology and Food Engineering at the Technion. Her research interests are at the broad interface between materials science and biotechnology with focus on development of novel nanomaterials for sensing, biosensing, bioassays, and advanced new drug delivery schemes.

## Figures

**Figure 1.** HRSEM images of a typical SCA. The cross-sectional micrograph depicting closely packed layer with a thickness of 5µm. Inset: a top view of the hexagonal nanostructure.

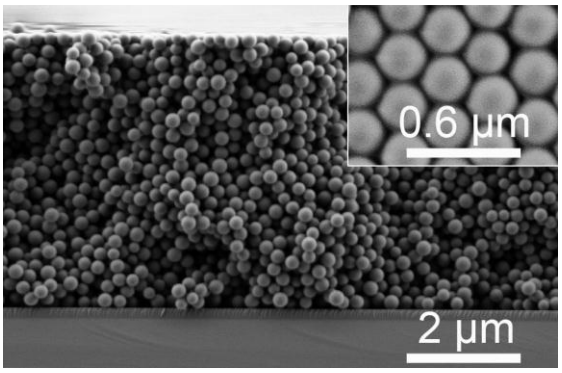


**Figure 2.** A schematic illustration of a reflectivity-based SCA sensing concept using a model analyte (i.e., EtOH). **(a)** Reflectivity spectra of a typical SCA, which are measured in air and EtOH (blue and red traces, respectively). **(b)** Fast Fourier transformation (FFT) of these spectra leads to single peaks, whose position and magnitude are monitored in real-time upon analyte solution introduction. Introduction of ethanol induces an increase the average refractive index of the porous structure, leading to a red-shift in the EOT value.

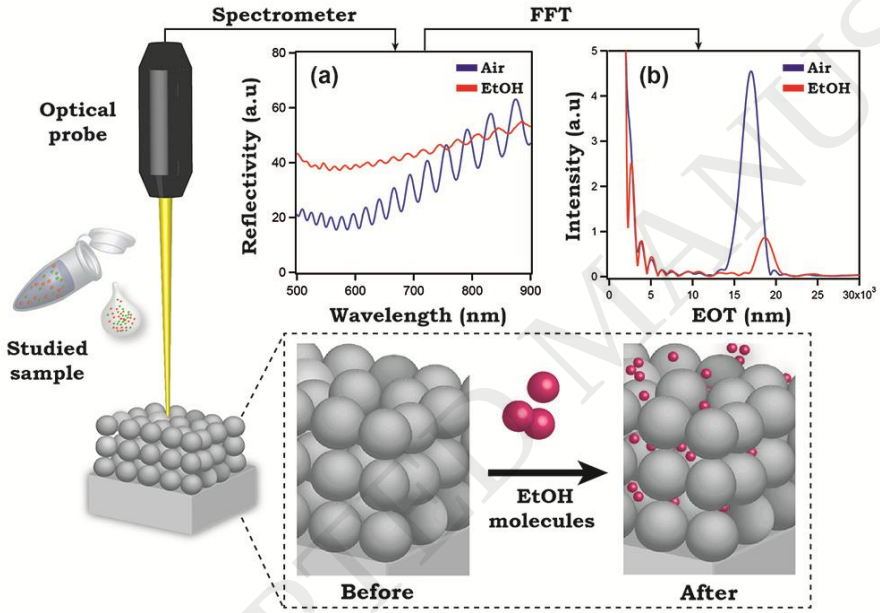


**Figure 3.** A schematic illustration of the synthetic steps followed for enzyme immobilization onto the SCA: **(a)** unmodified SCA; **(b)** APTES-modified surface; **(c)** GluAld-modified surface and **(d)** Trypsin-modified surface. Note: the enzymes were immobilized throughout the entire SCA scaffold surface. **(e)** The corresponding relative EOT changes upon the biofunctionalization steps onto SCA. Note: the EOT values obtained after each modification step were normalized with respect to the EOT value of the unmodified SCA (termed as $EOT_0$).

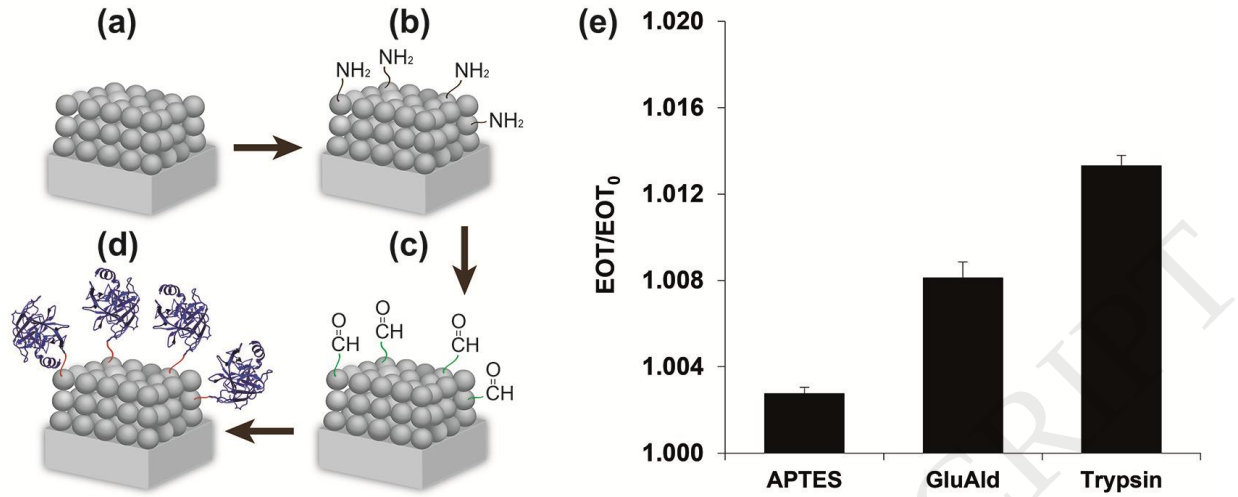


**Figure 4.** Confirmation of proteolytic activity of the SCA immobilized enzymes. CLSM 3D projection images of FTC-casein fragments after reaction with **(a)** trypsin-modified SCA and **(b)** HRP-modified SCA. The scale bar is 20 µm. **(c)** Fluorescence intensity values of the corresponding CLSM data obtained using the Imaris software. The porous film boundaries were validated by monitoring the blue signal ($\lambda_{em}$ = 405 nm) resulting from the photoluminescence of the oxidized nanostructure (data not shown). Note: the photoluminescence of the porous nanostructure results from the combination of quantum confinement effect and surface chemistry.

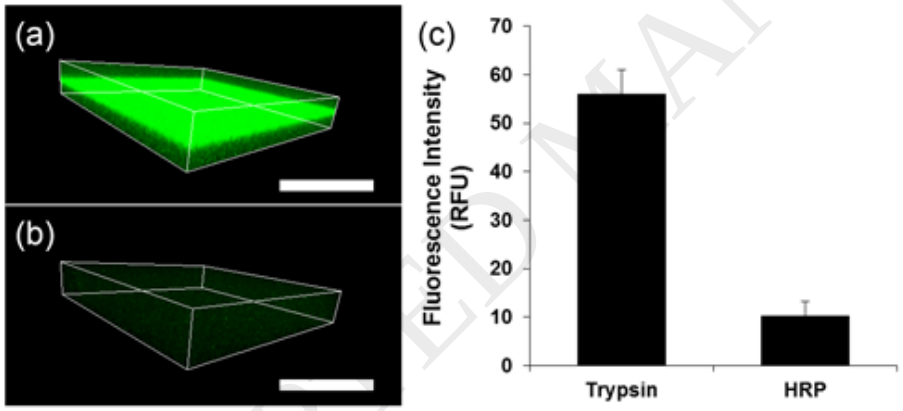


**Figure 5. (a)** Relative EOT changes upon enzymes (trypsin and HRP) biofunctionalization onto the SCA, proteolytic cleavage of myoglobin (after 1 and 2 h, respectively) and product retrieval by HEPES buffer wash. Note: the EOT values obtained after each modification step were normalized with respect to the EOT value of the unmodified SCA scaffold (termed as $EOT_0$). **(b)** Amino acid sequence of myoglobin after trypsin digestion. Sequences in red reflect the peptides identified by LC-MS/MS analysis. *Significantly different (t-test, $p$<0.05).